

Supporting Information

Tuning the ionic conduction and structure stability of ammonium vanadate by intercalating polyaniline molecular for advanced aqueous zinc-ion batteries

Liming Chen^a, Ziqiang Zhang^a, Yu Ma^a, Yuanming Wang^b, **, Huanhao Xiao^a, Ming Xu^a, Youyuan Huang^c, *** and Guohui Yuan^a, *

^a MIIT Key Laboratory of Critical Materials Technology for New Energy Conversion and Storage, School of Chemistry and Chemical Engineering, Harbin Institute of Technology, Harbin 150001, P. R. China

^b College of Bioresources Chemical and Materials Engineering, Shaanxi Provincial Key Laboratory of Papermaking Technology and Specialty Paper Development, National Demonstration Center for Experimental Light Chemistry Engineering Education, Shaanxi University of Science & Technology, Xi'an 710021, P. R. China

^c BTR New Material Group Co., Ltd., Shenzhen 518106, P. R. China

*Corresponding author at: School of Chemistry and Chemical Engineering, Harbin Institute of Technology, Harbin 150001, P. R. China

**Corresponding author at: College of Bioresources Chemical and Materials Engineering, Shaanxi University of Science & Technology, Xi'an 710021, P. R. China

***Corresponding author at: BTR New Material Group Co., Ltd., Shenzhen 518106, P. R. China

E-mail addresses: yghhit@163.com (G. Yuan), yminghit@163.com (Y. Wang),

huangyouyuan@btrchina.com (Y. Huang).

Electrochemical method

CV: The Zn^{2+} diffusion coefficient was calculated by the CV curves at different scanning rate, which was based on the following equation:

$$I_p = 2.695 \times 10^5 ACD^{1/2}n^{2/3}v^{1/2} \quad (S1)$$

Where I_p is the peak current of cathodic and anodic peaks, A is the area of electroactive material contact with electrolyte, C is the concentration of Zn^{2+} in electrode, D is the diffusion coefficient of Zn^{2+} , n represents the number of electrons transferred per molecule, v is the scan rate

GITT: The Galvanostatic and intermittent titration technique (GITT) was measured to investigate the solid-state diffusion kinetics of Zn^{2+} in the charging and discharge process. After discharged and charged for several cycles to stable state, the battery was discharged or charged about 10 min at 0.1 A g^{-1} , and followed relaxed for 60 min during the entire process. The Zn^{2+} diffusion coefficient was calculated by the above GITT data, which was based on the following equation:

$$D_{Zn^{2+}} = \frac{4}{\pi\tau} \left(\frac{m_B V_M}{M_B S} \right)^2 \left(\frac{\Delta E_s}{\Delta E_\tau} \right)^2 \quad (S2)$$

Where D is the diffusion coefficient of Zn^{2+} , τ is to the current pulse time of battery, m_B is the mass of the active material, M_B is the molecular weight ($g \text{ mol}^{-1}$) and V_M is the molar volume ($cm^3 \text{ mol}^{-1}$), S represents the surface area of electrode. The ΔE_τ and ΔE_s correspond to the voltage change of constant current pulse and the steady-state voltage change of the current pulse, respectively.

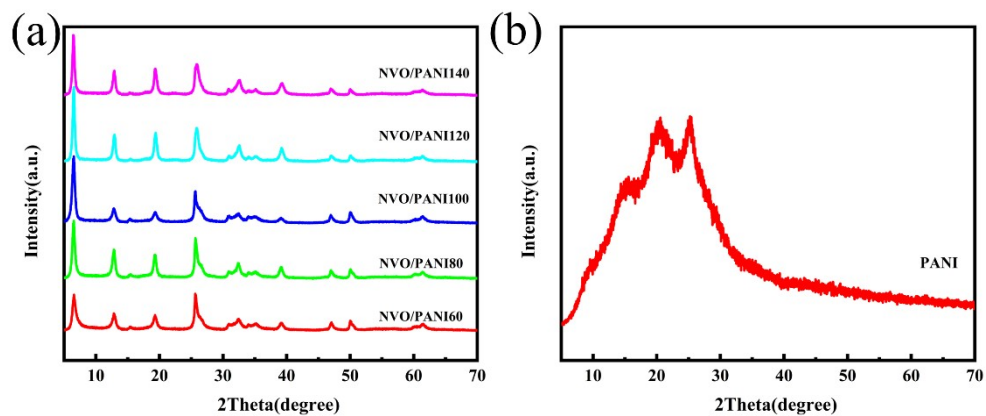


Fig. S1 (a) XRD patterns of NVO/PANI60, NVO/PANI80, NVO/PANI100, NVO/PANI120 and NVO/PANI140. (b) XRD pattern of pure PANI.

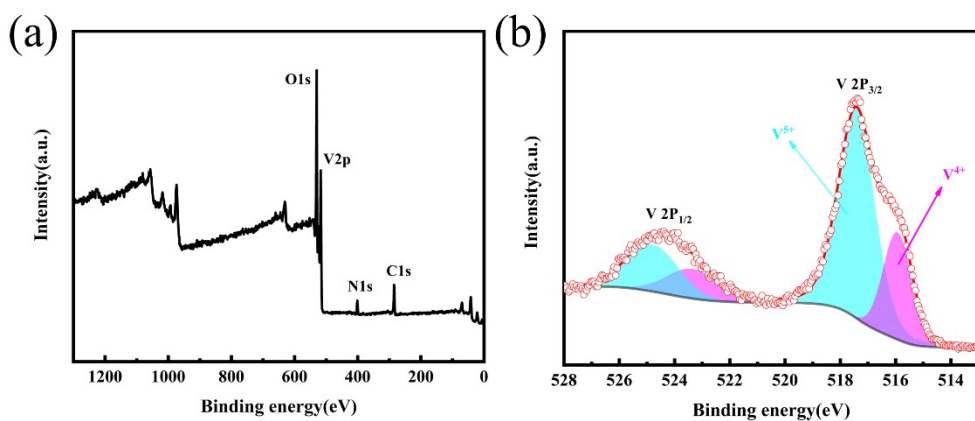


Fig. S2 (a) XPS spectra and (b) High-resolution spectra of V 2p of $\text{NH}_4\text{V}_4\text{O}_{10}$.

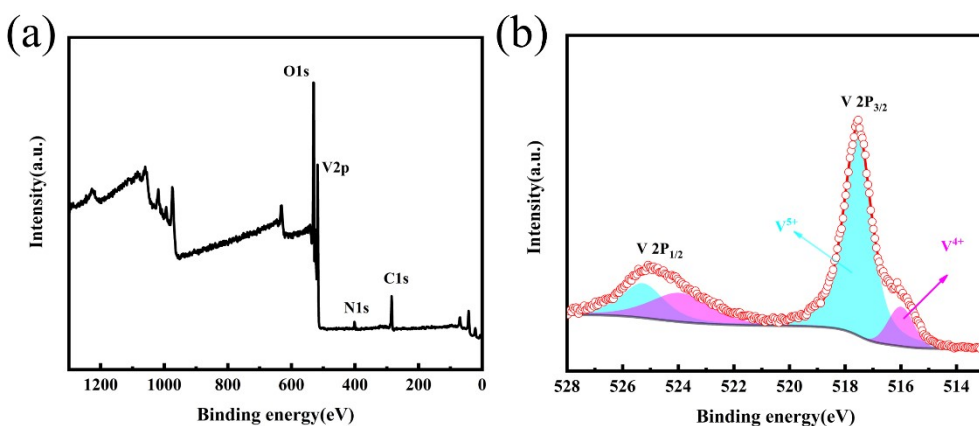


Fig. S3 (a) XPS spectra and (b) High-resolution spectra of V 2p of NVO without adding aniline.

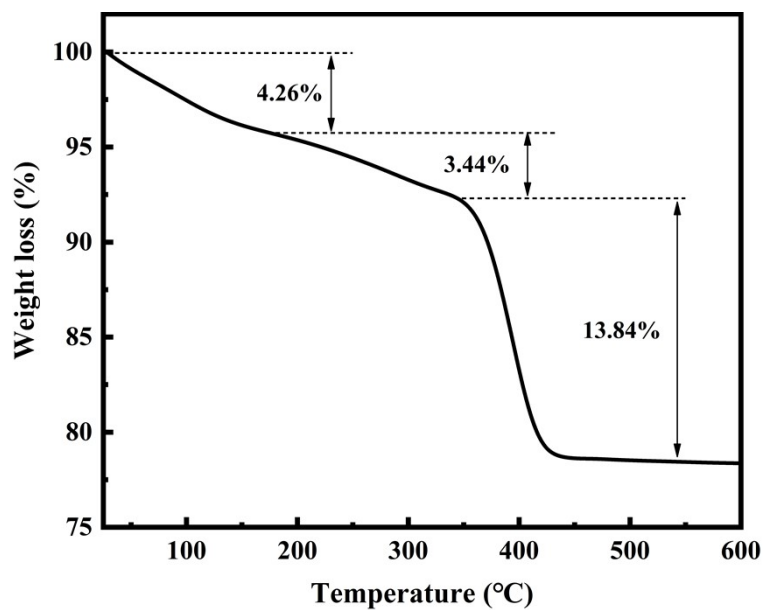


Fig. S4 The TG curve of NVO/PANI120.

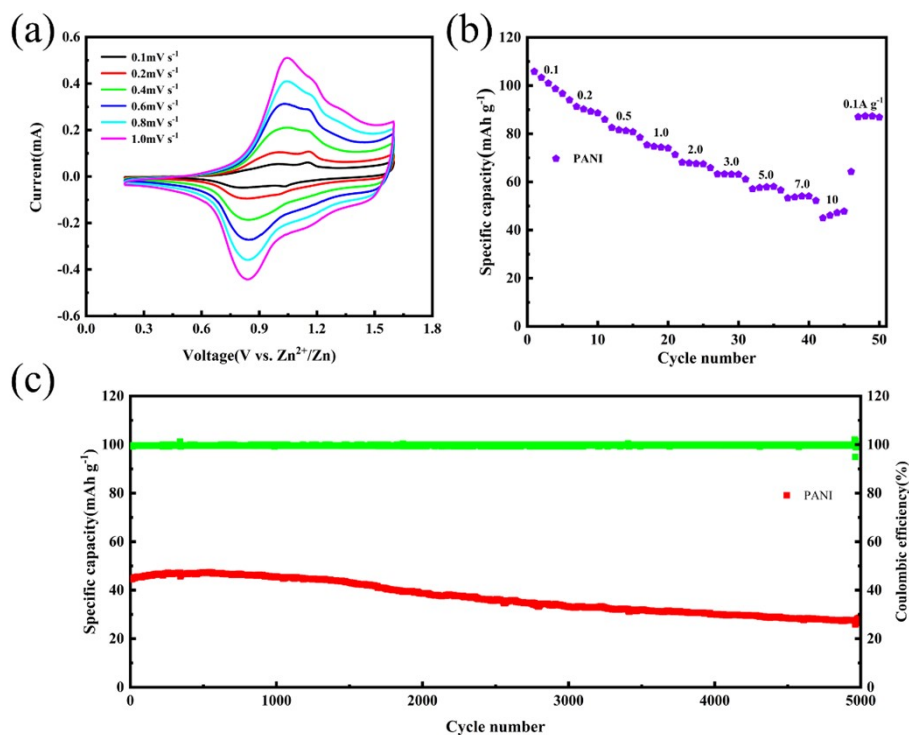


Fig. S5 (a) CV curves at various scan rates. (b) rate performance at different current densities and (c) cycling performance at 5 A g⁻¹ of the PANI.

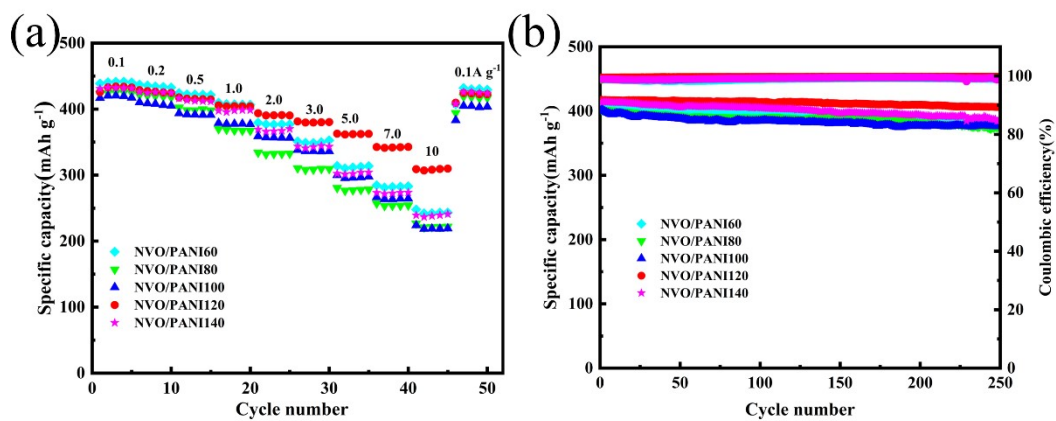


Fig. S6 (a) Rate performance and (b) cycling performance at 5 A g⁻¹ of NVO/PANI60,

NVO/PANI80, NVO/PANI100, NVO/PANI120 and NVO/PANI140.

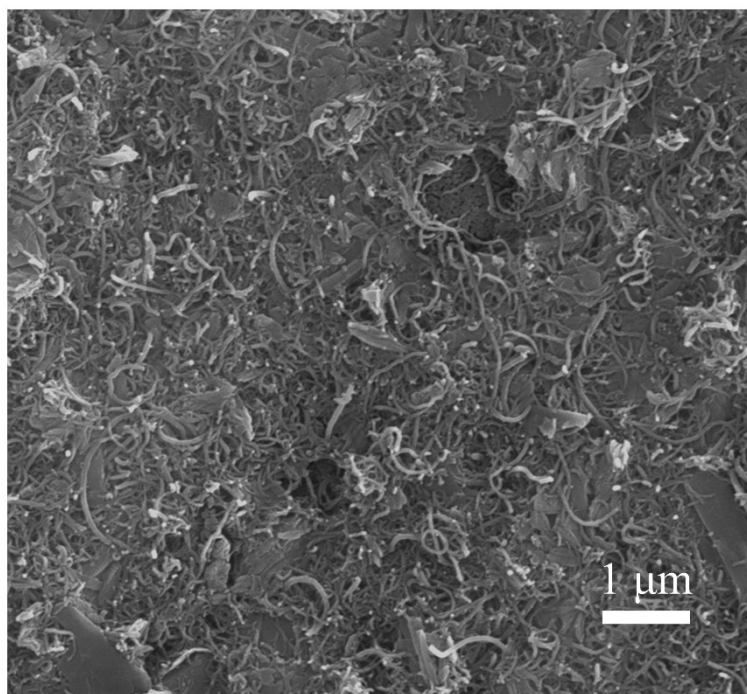


Fig. S7 The SEM image of NVO/PANI120 electrode at 0.1 A g⁻¹ after 100 cycles.

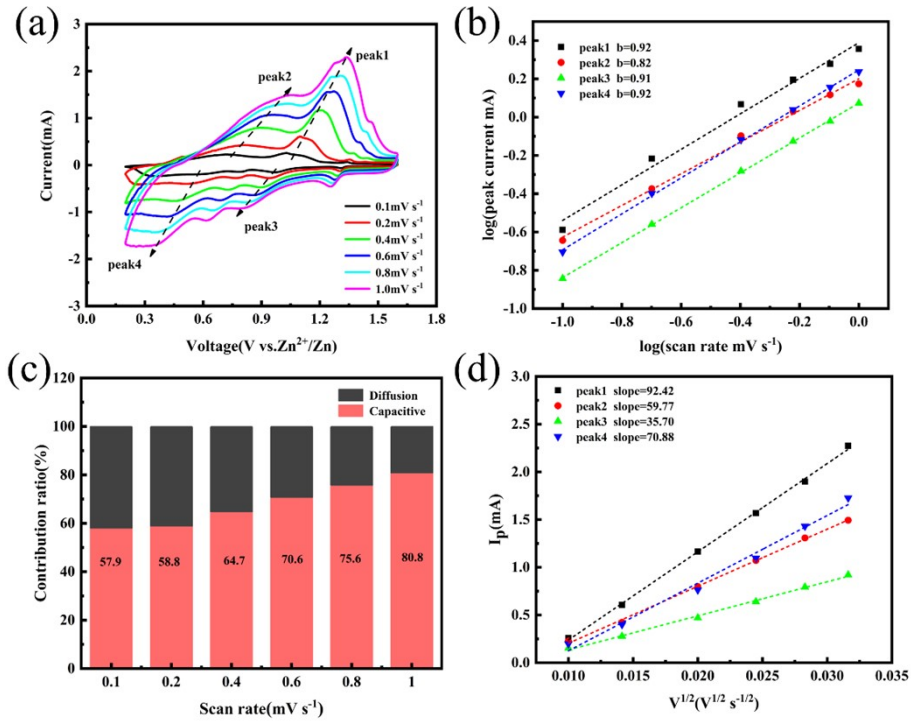


Fig. S8 (a) CV curves from 0.1 mV s^{-1} to 1.0 mV s^{-1} , (b) the relationship between peak currents and scan rate, (c) the percent of calculated capacitive contribution and (d) the linear relation of I_p and $v^{1/2}$ of $\text{NH}_4\text{V}_4\text{O}_{10}$ electrode.

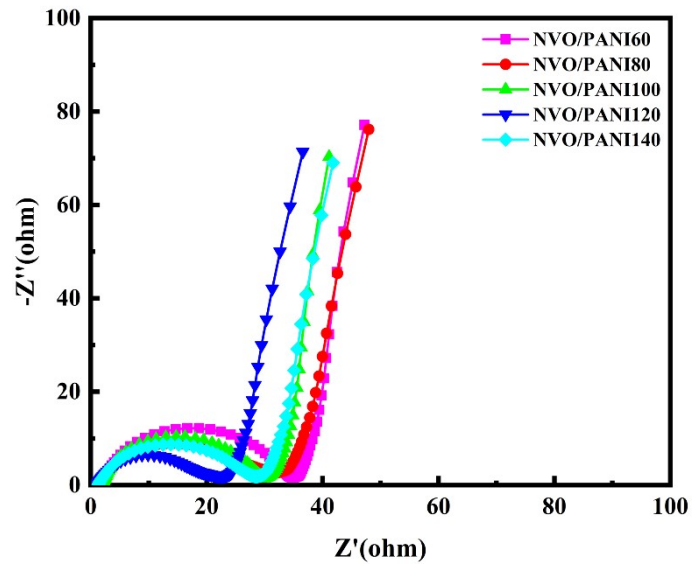


Fig. S9 Nyquist plots of $\text{NH}_4\text{V}_4\text{O}_{10}$, NVO/PANI60, NVO/PANI80, NVO/PANI100, NVO/PANI120 and NVO/PANI140.

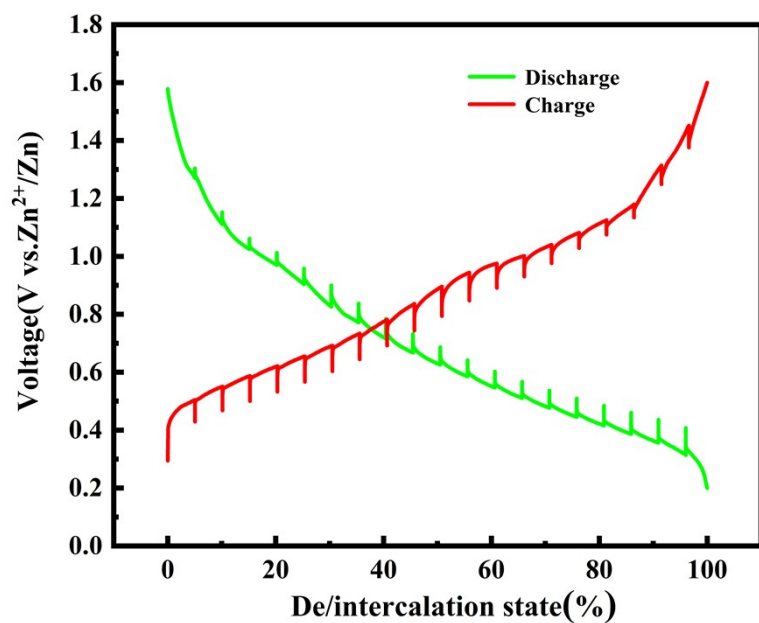


Fig. S10 GITT curves of the $\text{NH}_4\text{V}_4\text{O}_{10}$ electrode at 0.1 A g^{-1} .

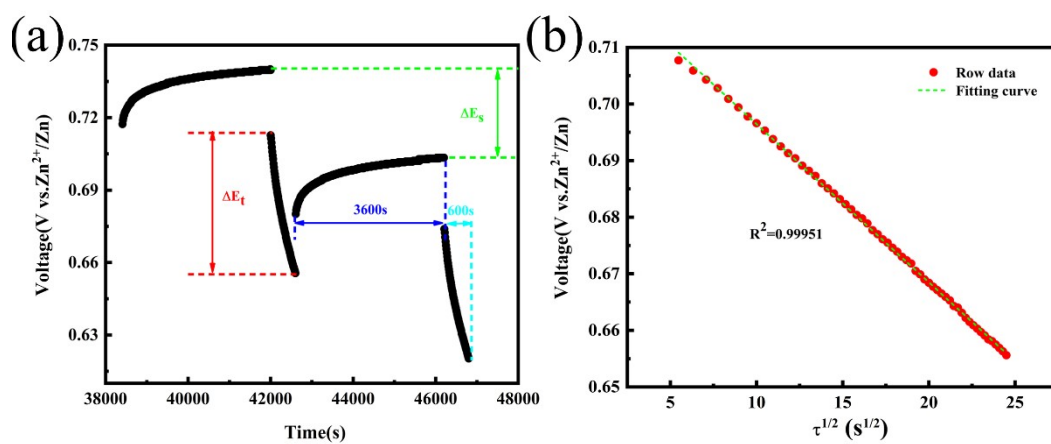


Fig. S11 (a) Schematic illustration of partial enlarged GITT curve and (b) the linear relationship

between E and $\tau^{1/2}$ at the discharge process for NVO/PANI120.

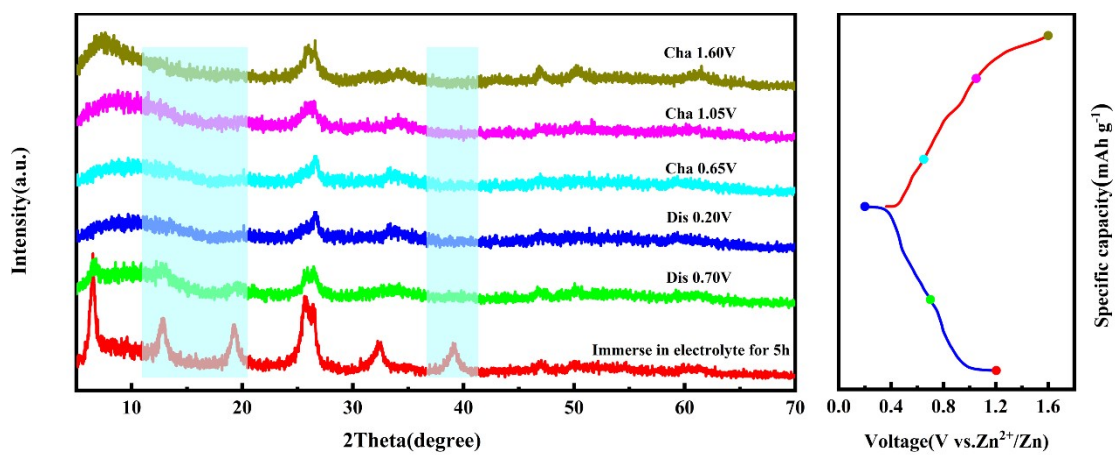


Fig. S12 The ex-situ XRD patterns of NVO/PANI120 during the first cycle.

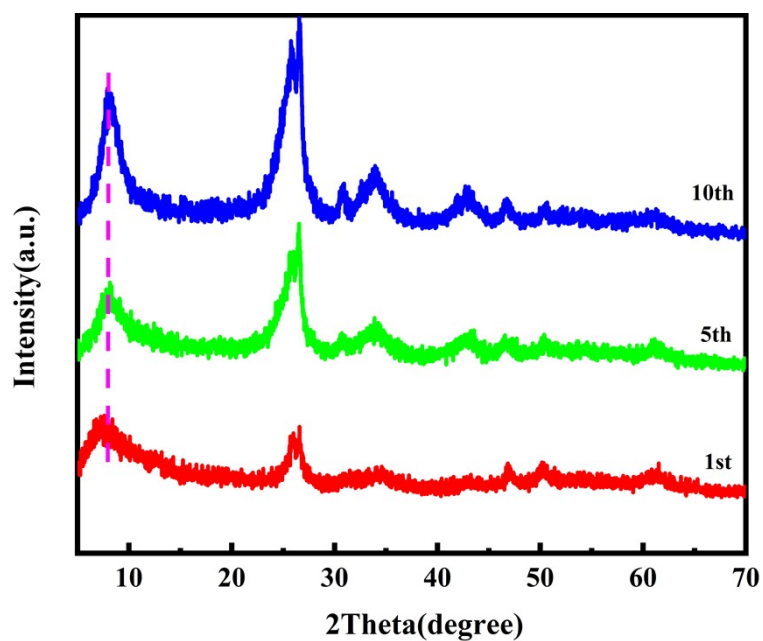


Fig. S13 XRD pattern of NVO/PANI at 1.6 V after different cycle number

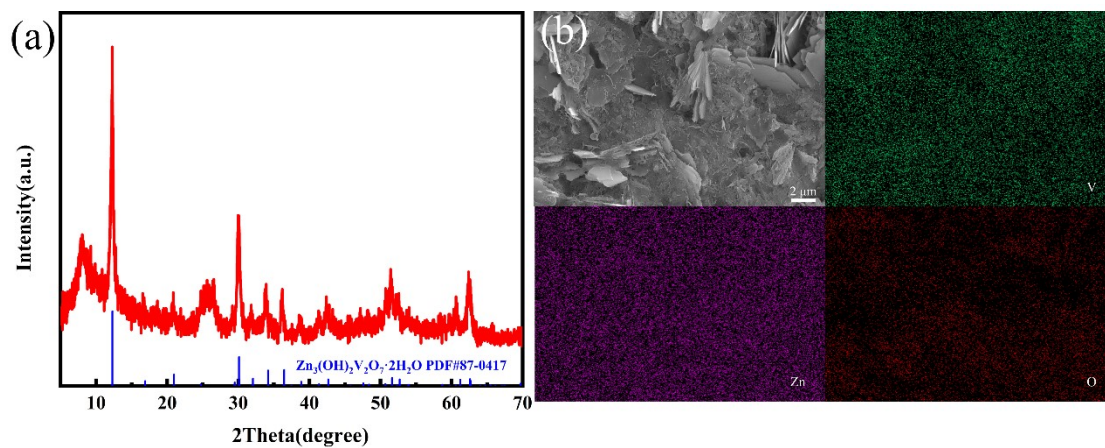


Fig. S14 (a) XRD pattern of NVO/PANI with discharging to 0.2 V, (b) the corresponding EDS

mapping.

Table S1. Electrochemical performances of V-based electrode materials of the aqueous zinc ion batteries.

Cathode	Electrolyte	Specific capacity	Rate performance	Cycling stability	Ref.
$(\text{NH}_4)_{0.5}\text{V}_2\text{O}_5$	2M ZnSO_4	418.4 mAh g ⁻¹ at 0.1 A g ⁻¹	223 mAh g ⁻¹ at 5 A g ⁻¹	91.4% retention after 2000 cycles at 5 A g ⁻¹	1
$\text{NH}_4\text{V}_4\text{O}_{10}$	3M $\text{Zn}(\text{CF}_3\text{SO}_3)_2$	475.8 mAh g ⁻¹ at 0.4 A g ⁻¹	142.5 mAh g ⁻¹ at 5 A g ⁻¹	90.0% retention after 2100 cycles at 5 A g ⁻¹	2
Oxygen-deficient $\text{NH}_4\text{V}_4\text{O}_{10}$	3M $\text{Zn}(\text{CF}_3\text{SO}_3)_2$	484.3 mAh g ⁻¹ at 0.1 A g ⁻¹	328.1 mAh g ⁻¹ at 3 A g ⁻¹	66.2% retention after 1000 cycles at 2 A g ⁻¹	3
Optimizing engineering $\text{NH}_4\text{V}_4\text{O}_{10}$	2M ZnSO_4	430 mAh g ⁻¹ at 0.1 A g ⁻¹	277.1 mAh g ⁻¹ at 10 A g ⁻¹	72.2% retention after 3000 cycles at 10 A g ⁻¹	4
$\text{NH}_4\text{V}_4\text{O}_{10}$	3M $\text{Zn}(\text{CF}_3\text{SO}_3)_2$	147 mAh g ⁻¹ at 0.05 A g ⁻¹	72 mAh g ⁻¹ at 2 A g ⁻¹	70.3% retention after 5000 cycles at 2 A g ⁻¹	5
Mo-doped $\text{NH}_4\text{V}_4\text{O}_{10}$	1M $\text{Zn}(\text{CF}_3\text{SO}_3)_2$	335 mAh g ⁻¹ at 0.1 A g ⁻¹	145.4 mAh g ⁻¹ at 2 A g ⁻¹	83.6% retention after 500 cycles at 0.5 A g ⁻¹	6
Ti-doped $\text{NH}_4\text{V}_4\text{O}_{10}$	3M $\text{Zn}(\text{CF}_3\text{SO}_3)_2$	298 mAh g ⁻¹ at 0.1 A g ⁻¹	143 mAh g ⁻¹ at 2 A g ⁻¹	89.0% retention after 2000 cycles at 2 A g ⁻¹	7
$\text{NH}_4\text{V}_4\text{O}_{10} \cdot 0.28\text{H}_2\text{O}$	2M $\text{Zn}(\text{CF}_3\text{SO}_3)_2$	410 mAh g ⁻¹ at 0.2 A g ⁻¹	112 mAh g ⁻¹ at 10 A g ⁻¹	76% retention after 500 cycles at 2 A g ⁻¹	8
Deficient $\text{NH}_4\text{V}_4\text{O}_{10}$	3M $\text{Zn}(\text{CF}_3\text{SO}_3)_2$	457 mAh g ⁻¹ at 0.1 A g ⁻¹	170 mAh g ⁻¹ at 5 A g ⁻¹	81.0% retention after 1000 cycles at 2 A g ⁻¹	9

Carbon fiber/ NH ₄ V ₄ O ₁₀	2M ZnSO ₄	434 mAh g ⁻¹ at 0.5 A g ⁻¹	140 mAh g ⁻¹ at 20 A g ⁻¹	83.0% retention after 2500 cycles at 20 A g ⁻¹	10
3D- NH ₄ V ₄ O ₁₀	1M Zn(ClO ₄) ₂	485 mAh g ⁻¹ at 0.1 A g ⁻¹	142 mAh g ⁻¹ at 10 A g ⁻¹	80.6% retention after 3000 cycles at 10 A g ⁻¹	11
NVO/PANI	3M Zn(CF ₃ SO ₃) ₂	433.8 mAh g ⁻¹ at 0.1 A g ⁻¹	308.06 mAh g ⁻¹ at 10 A g ⁻¹	92.23% retention after 5000 cycles at 5 A g ⁻¹	This work

Table S2. The charge transfer resistivities (R_{ct}) of NVO/PANI120 and reported cathode.

Samples	R_{ct} (initial cycle)	R_{ct} (after the cycle)	Reference
3D-NH ₄ V ₄ O ₁₀	35.17Ω	27Ω	2
NH ₄ V ₄ O ₁₀ -Na	143Ω	105Ω	12
NH ₄ V ₄ O ₁₀ -Ti	121.5Ω	62Ω	7
V ₂ O ₅ -PANI	24.1Ω	15.4	13
V ₂ O ₅ -Al	230.3Ω	53.04Ω	14
NVO/PANNI120	111.5 Ω	17.6 Ω	This work

References

1. D. Bin, Y. Liu, B. Yang, J. Huang, X. Dong, X. Zhang, Y. Wang and Y. Xia, Engineering a high-energy-density and long lifespan aqueous zinc battery via ammonium vanadium bronze, *ACS Appl. Mater. Inter.*, 2019, **11**, 20796-20803.
2. R. Sun, Z. Qin, X. Liu, C. Wang, S. Lu, Y. Zhang and H. Fan, Intercalation mechanism of the ammonium vanadate ($\text{NH}_4\text{V}_4\text{O}_{10}$) 3D decussate superstructure as the cathode for high-performance aqueous zinc-ion batteries, *ACS. Sustain. Chem. Eng.*, 2021, **9**, 11769-11777.
3. T. He, Y. Ye, H. Li, S. Weng, Q. Zhang, M. Li, T. Liu, J. Cheng, X. Wang, J. Lu and B. Wang, Oxygen-deficient ammonium vanadate for flexible aqueous zinc batteries with high energy density and rate capability at $-30\text{ }^\circ\text{C}$, *Mater. Today*, 2021, **43**, 53-61.
4. C. Huang, S. Liu, J. Feng, Y. Wang, Q. Fan, Q. Kuang, Y. Dong and Y. Zhao, Optimizing engineering of rechargeable aqueous zinc ion batteries to enhance the zinc ions storage properties of cathode material, *J. Power Sources*, 2021, **490**, 229528.
5. G. Yang, T. Wei and C. Wang, Self-healing lamellar structure boosts highly stable zinc-storage property of bilayered vanadium oxides, *ACS Appl. Mater. Inter.*, 2018, **10**, 35079-35089.
6. H. Wang, R. Jing, J. Shi, M. Zhang, S. Jin, Z. Xiong, L. Guo and Q. Wang, Mo-doped $\text{NH}_4\text{V}_4\text{O}_{10}$ with enhanced electrochemical performance in aqueous Zn-ion batteries, *J. Alloy. Compd.*, 2021, **858**, 158380.

7. D. He, Y. Peng, Y. Ding, X. Xu, Y. Huang, Z. Li, X. Zhang and L. Hu, Suppressing the skeleton decomposition in Ti-doped $\text{NH}_4\text{V}_4\text{O}_{10}$ for durable aqueous zinc ion battery, *J. Power Sources*, 2021, **484**, 229284.
8. T. Zhu, B. Mai, P. Hu, Z. Liu, C. Cai, X. Wang and L. Zhou, Ammonium Ion and Structural Water Co-Assisted Zn^{2+} Intercalation/De-Intercalation in $\text{NH}_4\text{V}_4\text{O}_{10} \cdot 0.28\text{H}_2\text{O}$, *Chinese. J. Chem.*, 2021, **39**, 1885-1890.
9. Q. Zong, W. Du, C. Liu, H. Yang, Q. Zhang, Z. Zhou, M. Atif, M. Alsalhi and G. Cao, Enhanced Reversible Zinc Ion Intercalation in Deficient Ammonium Vanadate for High-Performance Aqueous Zinc-Ion Battery, *Nano. Micro. Lett.*, 2021, **13**, 116.
10. M. Tamilselvan, T. V. M. Sreekanth, K. Yoo and J. Kim, Ultrathin ammonium vanadate nanoflakes on carbon fiber – A binder-free high-rate capability cathode for aqueous medium zinc ion storage, *J. Alloy. Compd.*, 2021, **876**, 160130.
11. Q. Li, X. Rui, D. Chen, Y. Feng, N. Xiao, L. Gan, Q. Zhang, Y. Yu and S. Huang, A High-Capacity Ammonium Vanadate Cathode for Zinc-Ion Battery, *Nano. Micro. Lett.*, 2020, **12**, 67.
12. X. Wang, A. Naveed, T. Zeng, T. Wan, H. Zhang, Y. Zhou, A. Dou, M. Su, Y. Liu and D. Chu, Sodium ion stabilized ammonium vanadate as a high-performance aqueous zinc-ion battery cathode, *Chem. Eng. J.*, 2022, **446**, 137090.
13. S. Liu, H. Zhu, B. Zhang, G. Li, H. Zhu, Y. Ren, H. Geng, Y. Yang, Q. Liu and C. C. Li, Tuning the kinetics of zinc-ion insertion/extraction in V_2O_5 by in situ polyaniline intercalation enables improved aqueous zinc-ion storage performance,

Adv. Mater., 2020, **32**, 2001113.

14. H. Jiang, W. Gong, Y. Zhang, X. Liu, M. Waqar, J. Sun, Y. Liu, X. Dong, C. Meng, Z. Pan and J. Wang, Quench-tailored Al-doped V₂O₅ nanomaterials for efficient aqueous zinc-ion batteries, *J. Energy Chem.*, 2022, **70**, 52-58.